McMaster University

Advanced Optimization Laboratory

Title:

Simulation of steady-state NMR of coupled systems using Liouville space and computer algebra methods

Author:

Christopher Kumar Anand, Alex Bain, Zhenghua Nie

AdvOL-Report No. 2007/6

June, 2007
Hamilton, Ontario, Canada

Simulation of Steady-State NMR of Coupled Systems Using Liouville Space and Computer Algebra Methods

Christopher Kumar Anand [a] Alex D. Bain [b,*] Zhenghua Nie [c]

[a] *Department of Computing and Software*
[b] *Department of Chemistry*
[c] *School of Computational Engineering and Science*
McMaster University

Abstract

A series of repeated pulses and delays applied to a spin system generates a steady state. This is relatively easy to calculate for a single spin, but coupled systems present real challenges. We have used Maple, a computer algebra program to calculate one- and two-spin systems symbolically, and larger systems numerically. The one-spin calculations illustrate and validate the methods and show how the steady-state free precession method converges to continuous wave NMR. For two-spin systems, we have derived a general formula for the creation of double-quantum signals as a function of irradiation strength, coupling constant, and chemical shift difference. The calculations on three-spin and larger systems reproduce and extend previously published results. In this paper, we have shown that the approach works well for systems in the literature. However, the formalism is general and can be extended to more complex spin systems and pulses sequences.

Key words: steady state, pulsed NMR, continuous wave NMR, multiple quantum transitions, Liouville space methods, computer algebra program

* Department of Chemistry, McMaster University, 1280 Main St. West, Hamilton, Ontario Canada L8S 4M1
Email address: bain@mcmaster.ca (Alex D. Bain).

1 Introduction

Part of pulsed NMR can be considered a set of methods for creating "interesting" spin density matrices. The density matrix, and its time dependence, contain all possible information about the spin system: both the experiments and their theoretical analysis involve manipulations of the density matrix to extract the information we need. In the majority of cases, we assume that the spin system starts at equilibrium, then we apply a series of pulses and delays, and acquire our data. This is not the case in MR imaging, in which steady-state methods have become widespread. The goal of this paper is to derive and test methods for applying these steady-state methods to much more complex spin systems.

Steady-state in this context means that the spin system is subjected to a continual series of pulses, delays and data acquisition periods. Rather than the spin system returning to equilibrium after each acquisition, it is kept in a potentially more interesting steady state. Both the pulse sequence and spin relaxation determine the state, whereas relaxation is much less important in standard pulse sequence design. In medical imaging, these steady-state methods lead to much faster acquisitions [1,2,3], even to real-time images. Since the bulk of this work is aimed at anatomical or relaxation-weighted images, most of the analysis of steady-state experiments has been based on a single spin system, which can be described by the Bloch equations [4,5,6,7,8].

The goal of this paper is to explore steady-state methods in systems of coupled spins. Homonuclear spin coupling remarkably complicates the spin dynamics of these systems, but modern methods, such as Liouville-space techniques and computer algebra programs can make this manageable. One aspect of the steady-state free-precession (SSFP) method has already been analyzed and applied to coupled spin systems, in the form of continuous wave (CW) methods [9], which are the limit of the SSFP technique. In SSFP, short pulses are alternated with small delays during which a data point [1] is acquired. The radio frequency power of the pulse, averaged over both the pulse width and the delay, becomes the analogy of the CW power. As the transmitter frequency is swept, a spectrum identical to the CW spectrum is obtained, in the limit of low power and short delay.

At higher power, a CW spectrum of a coupled spin system will not only show the expected saturation broadening (as in a single spin case), but it will also produce multiple-quantum peaks [10]. If we have two spins, then at sufficiently high power, a sharp peak at the average of the two Larmor frequencies will appear in the CW spectrum. Further power increases will broaden and saturate

[1] In MR *Imaging*, multiple points are acquired, but we frame the discussion in terms of NMR spectroscopy *without gradients* in this paper.

this line. The approximate behaviour of multiple-quantum transitions in a two-spin system has been derived theoretically [11], and three-spin systems have been treated numerically [12,13,14]. We can use the established SSFP analogy and the multiple-quantum work to validate and test our more powerful approach.

In this paper, we re-derive the formal set of equations in Liouville space to calculate the steady-state density matrix. We can include a continuous rf field, to calculate the CW spectrum for any values of the parameters. However, a much more powerful approach is to embed a pulse sequence into the formulation. The same formalism can then be used to calculate the steady-state created by a more complex pulse sequence with explicit pulses and delays. For this paper, we apply only the simple pulse-delay SSFP sequence, but there is nothing in the theory that restricts us to this experiment. Future papers will explore more complex pulse sequences.

For a single spin, the Liouville system corresponds to the Bloch equations, and the calculations are easy. We use the computer algebra program Maple [2] to symbolically derive the CW solution. Next, we derive the symbolic SSFP solution, and show how the pulse flip angle and the delay are combined to provide the same effect as the CW field. This can be done exactly, or in an approximate fashion, in which the delay is assumed to be small compared to the relaxation times and the time associated with the offset between the rf and the Larmor frequency. This approximate solution converges to the CW solution, and represents the SSFP experiment.

For two spins, the calculation is considerably more difficult. As well as the rf power, we now must consider the chemical shift difference and the coupling constant. There are some approximate analytical calculations of the double-quantum intensity [11], which we are able to derive and extend symbolically. We also use Maple to explore this spectroscopy numerically, in order to get a feeling for how a coupled spin system responds. For three or more spins, symbolic calculations are out of the question, but numerical calculations are certainly feasible. Worvill [14] had looked at the response of a three-spin system, in order to test whether it was sensitive to the exact nature of the relaxation mechanism. This work was not pursued much further, but is an example of what we wish to do in the future.

Finally, since the interplay of pulse sequence, spin system and relaxation behaviour is more complex than in standard pulse sequence design, optimization methods will be applied in future work to improve the experiments. In this way, we hope to find new and efficient ways of creating desirable (and perhaps otherwise inaccessible) configurations of the density matrix by steady-state

[2] http://www.maplesoft.com/

h

$\|0)$	$= \frac{1}{\sqrt{2}}\mathbf{1}$
$\|1_{+1})$	$= -(\mathbf{I}_x + i\mathbf{I}_y)$
$\|1_0)$	$= \sqrt{2}\mathbf{I}_z$
$\|1_{-1})$	$= (\mathbf{I}_x - i\mathbf{I}_y)$

Table 1
Spherical tensor basis for the Liouville Space of a single spin-$\frac{1}{2}$.

methods.

2 Liouville Space Formulation

The density matrix encodes all possible information about a spin system and the measurements we can make to extract that information. We use the Liouville space method [15] to represent the density matrix and determine solutions of the continuous wave and pulsed NMR experiments.

In this paper, $|0)$, $|1_{+1})$, $|1_0)$ and $|1_{-1})$ represent the four observables for one single spin-$\frac{1}{2}$ system in the Liouville space, see Table 1, following the notation of Bain [15].

These observables form a basis for a single spin system,

$$\{|0), |1_{+1}), |1_0), |1_{-1})\}\,, \tag{1}$$

and combine to form bases for multiple spin-$\frac{1}{2}$ systems by using direct products of the single spin system basis.

The density operator is a vector in Liouville space and the equation of motion for the density matrix vectors is expressed as

$$\partial\rho/\partial t = -i\mathcal{L}\rho - \mathcal{R}(\rho - \rho_{\mathrm{eq}}), \tag{2}$$

where ρ is the state vector of the spin system and ρ_{eq} is the equilibrium state, $\mathcal{L}$ is the Liouvillian matrix encoding information about Larmor frequencies, chemical structure and couplings (if the spin system is multiple), and $\mathcal{R}$ is the relaxation matrix. Please note that $i\mathcal{L}\rho_{\mathrm{eq}} = 0$.

In the Liouville space, observables are detected by taking the dot (scalar) product between two Liouville space vectors. This is equivalent to the trace product in the operator formalism [15,16], *i.e.*

$$(P|Q) = \mathrm{trace}(\hat{P}\hat{Q}), \tag{3}$$

where on the left hand side, P and Q are Liouville Space vectors, whereas the right hand side $\hat{P}$ and $\hat{Q}$ denote Hilbert space operators. We can only detect the single quantum signal, which is $|1_{+1}\rangle$ in our basis, representing the total x-y magnetization precessing in the positive direction.

2.1 General Solution for the Continuous Wave Case

In continuous wave (CW) NMR experiments, a continuous radio frequency field, B_1, is applied, making the evolution

$$\partial\rho/\partial t = -i(\mathcal{L} + \mathcal{B})\rho - \mathcal{R}(\rho - \rho_{\mathrm{eq}}) \tag{4}$$

where $\mathcal{B}$ is the matrix for the effect of the rf field B_1. The next section will give these matrices for a single spin system. Because $|0\rangle$, the total number of spins, is a constant, we only consider the parts ($|1_{+1}\rangle$, $|1_0\rangle$ and $|1_{-1}\rangle$) of these matrices in the computation. These components represent the x-y and z magnetization.

At steady state,

$$\partial\rho/\partial t = 0. \tag{5}$$

Considering Eqs. (4) and (5), we get the general expression for calculating the steady state:

$$\rho_{\mathrm{SS}} = (i(\mathcal{L} + \mathcal{B}) + \mathcal{R})^{-1}\mathcal{R}\rho_{\mathrm{eq}} \tag{6}$$

We can solve the single spin system symbolically using Maple library functions. For two-spin systems, such general methods fail, and we have written our own Gaussian elimination procedures designed using knowledge of the structure of the Liouvillians to keep intermediate symbolic expressions from exploding. For arbitrary systems, we need to use numerical methods.

2.2 General Solution for the Pulsed Case

We consider pulsed NMR experiments composed of hard pulses and delays. In the first case we can ignore precession and relaxation ($\mathcal{L} = \mathcal{R} = 0$), and in the second there is no rf field ($B_1 = 0$). We solve the corresponding reduced systems separately.

The effect of a hard pulse is equivalent to a rotation of the reference frame. A rotation for spherical tensors is defined by a special matrix called a Wigner rotation matrix [17] and the direct product provides the rotation for multiple

spins. The following equation gives the effect of a hard pulse:

$$\rho_+ = W(\alpha)\rho_- \tag{7}$$

where ρ_- is the state before the pulse, ρ_+ is the state after the pulse, $W(\alpha)$ is the rotation matrix around the y-axis, α is the flip angle which is related to the strength of the radio frequency field B_1. Hard pulses correspond to the limit in which $\gamma B_1 \to \infty$ and *pulse width* $\to 0$, but the flip angle α remains constant.

For short delays, we have the following approximation:

$$\gamma B_1 \approx \frac{\alpha}{T_{\mathrm{R}}} \tag{8}$$

where T_{R} is the delay time.

Fig. 1 displays the simplest steady state pulse sequence. At each time point,

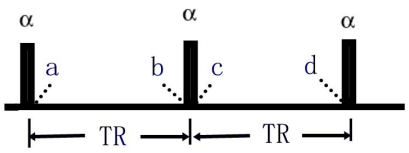

Figure 1. The simplest pulsed NMR experiment

we can calculate the spin states $\rho_{\mathrm{a}}, \rho_{\mathrm{b}}, \rho_{\mathrm{c}}, \rho_{\mathrm{d}}$. When the spin system is at the steady state, $\rho_{\mathrm{a}} = \rho_{\mathrm{c}}$ and $\rho_{\mathrm{b}} = \rho_{\mathrm{d}}$. We can use equations for the spin dynamics to relate spin states in different repeat times, and then solve these equations for the steady-state value. In this paper, the measured signal is ρ_{b} which is corresponded to the echo signal in [18]. Gyngell [18] and Hanicke & Vogel [3] discuss the solution of a single spin system at the time point a and b. In this paper, we give a general full expression and general approximate expression for an SSFP experiment on a system of n spins.

In order to calculate the spin states at different time points, we need to solve Eq. (2). Considering the fact that $i\mathcal{L}\rho_{\mathrm{eq}} = 0$, Eq. (2) can be reformulated as:

$$\frac{d}{dt}(\rho - \rho_{\mathrm{eq}}) = (-i\mathcal{L} - \mathcal{R})(\rho - \rho_{\mathrm{eq}}) \tag{9}$$

So the principal solution of Eq. (2) is:

$$\rho(t) = e^{-(i\mathcal{L}+\mathcal{R})t}(\rho_0 - \rho_{\mathrm{eq}}) + \rho_{\mathrm{eq}} \tag{10}$$

where ρ_0 is the state at time $t = 0$ which is the initial state when the delay starts.

Based on Fig. 1, the states ρ_{a}, ρ_{b}, and ρ_{c} are related by affine equations:

$$\rho_{\mathrm{b}} = e^{-(i\mathcal{L}+\mathcal{R})T_{\mathrm{R}}}(\rho_{\mathrm{a}} - \rho_{\mathrm{eq}}) + \rho_{\mathrm{eq}} \tag{11}$$
$$\rho_{\mathrm{c}} = W(\alpha)\rho_{\mathrm{b}} \tag{12}$$

where T_{R} is the repeat time—the time between successive pulses.

Because ρ_{c} is equal to ρ_{a} at the steady state, solving Eqs. (11) and (12), we get the general analytic solution for SSFP experiments:

$$\rho_{\mathrm{b}} = (\mathbf{1} - e^{-(i\mathcal{L}+\mathcal{R})T_{\mathrm{R}}}W(\alpha))^{-1}(\mathbf{1} - e^{-(i\mathcal{L}+\mathcal{R})T_{\mathrm{R}}})\rho_{\mathrm{eq}} \tag{13}$$

where $\mathbf{1}$ is an identity matrix which has the same size as the Liouvillian matrix and the relaxation matrix.

It is difficult to calculate ρ_{b} symbolically for a multiple spin system using Eq. (13). We will give the symbolic solution ρ_{b} for a single spin system and use Eq. (13) in the numerical computation for multiple-spin systems.

In order to analyze SSFP and discover the relationship between parameters such as the repeat time, relaxation times, Larmor frequencies, and others, we use the following equation to approximately calculate ρ_{b} when the repeat time of pulses is very short:

$$\partial\rho/\partial t \approx \frac{\rho_{\mathrm{b}} - \rho_{\mathrm{a}}}{T_{\mathrm{R}}} \tag{14}$$

Replacing the left side of Eq. (2), we get a new equation:

$$\frac{\rho_{\mathrm{b}} - \rho_{\mathrm{a}}}{T_{\mathrm{R}}} \approx -i\mathcal{L}\rho_{\mathrm{b}} - \mathcal{R}(\rho_{\mathrm{b}} - \rho_{\mathrm{eq}}) \tag{15}$$

Solving Eqs. (15) and (12), ρ_{b} is expressed:

$$\rho_{\mathrm{b}} \approx T_{\mathrm{R}}(\mathbf{1} + (i\mathcal{L} + \mathcal{R})T_{\mathrm{R}} - W(\alpha))^{-1}\mathcal{R}\rho_{\mathrm{eq}} \tag{16}$$

The above equation is the general approximate expression for an SSFP experiment on a system of n spins. Comparing Eq. (13) and Eq. (16) , it is cheaper to calculate ρ_{b} using Eq. (16) which does not require the computation of the exponential of a complex matrix.

3 Solutions of a single spin-$\frac{1}{2}$ system

Firstly, we list each matrix for a single spin system in our calculation. All of these matrices are constructed in the basis Eq. (1).

The Liouvillian matrix of a single spin-$\frac{1}{2}$ system is:

$$\mathcal{L} = \begin{pmatrix} 0 & 0 & 0 & 0 \\ 0 & \Delta\omega & 0 & 0 \\ 0 & 0 & 0 & 0 \\ 0 & 0 & 0 & -\Delta\omega \end{pmatrix} \tag{17}$$

where $\Delta\omega$ is the resonance offset $(\omega - \omega_0)$, and ω_0 is the centre frequency.

The relaxation matrix of a single spin-$\frac{1}{2}$ system is:

$$\mathcal{R} = \begin{pmatrix} 0 & 0 & 0 & 0 \\ 0 & \frac{1}{T_2} & 0 & 0 \\ 0 & 0 & \frac{1}{T_1} & 0 \\ 0 & 0 & 0 & \frac{1}{T_2} \end{pmatrix} \tag{18}$$

where T_1 and T_2 are the spin-lattice and spin-spin relaxation times.

The $\mathcal{B}$ matrix for the effect of CW acting on a single spin-$\frac{1}{2}$ system along the x-axis is:

$$\mathcal{B} = \begin{pmatrix} 0 & 0 & 0 & 0 \\ 0 & 0 & -\frac{1}{\sqrt{2}}\gamma B_1 & 0 \\ 0 & -\frac{1}{\sqrt{2}}\gamma B_1 & 0 & \frac{1}{\sqrt{2}}\gamma B_1 \\ 0 & 0 & \frac{1}{\sqrt{2}}\gamma B_1 & 0 \end{pmatrix} \tag{19}$$

where γ is the gyromagnetic ratio and B_1 is the strength of the radio-frequency.

The rotation matrix, which rotates around the y-axis, for the effect of a pulse acting on a single spin-$\frac{1}{2}$ system in the Liouville space is:

$$W(\alpha) = \begin{pmatrix} 1 & 0 & 0 & 0 \\ 0 & (\cos(\alpha/2))^2 & \frac{1}{\sqrt{2}}\sin(\alpha) & (\sin(\alpha/2))^2 \\ 0 & -\frac{1}{\sqrt{2}}\sin(\alpha) & \cos(\alpha) & \frac{1}{\sqrt{2}}\sin(\alpha) \\ 0 & (\sin(\alpha/2))^2 & -\frac{1}{\sqrt{2}}\sin(\alpha) & (\cos(\alpha/2))^2 \end{pmatrix} \tag{20}$$

where α is the flip angle.

All of matrices $\mathcal{L}$, $\mathcal{R}$, $\mathcal{B}$ and W are 4-by-4 which corresponds to the basis Eq. (1). As we said before, in order to avoid singular matrices, we only consider

the subspace spanned by $\{|1_{+1}), |1_0), |1_{-1})\}$ in the computation. When we set up multiple spin-$\frac{1}{2}$ systems, we need to take direct-products of 4-by-4 matrices first, before eliminating the total magnetization component.

Often, the equilibrium is given as:

$$\rho_{\text{eq}} = \begin{pmatrix} 0 \\ 1 \\ 0 \end{pmatrix}$$

but in this paper, we use

$$\rho_{\text{eq}} = \begin{pmatrix} 0 \\ \sqrt{2}M_0 \\ 0 \end{pmatrix}$$

to facilitate symbolic comparisons between CW and SSFP.

3.1 Single-spin CW Solution

Substituting the matrices in Eqs. (17), (18), and (19) for a single spin system into Eq. (6), and applying the detection method from Eq. (3), we get the measured signal s in the x-y plane:

$$s = M_0 \frac{\gamma B_1 (\Delta\omega T_2 + i) T_2}{1 + (\Delta\omega)^2 T_2^2 + (\gamma B_1)^2 T_1 T_2}, \tag{21}$$

which has real and imaginary parts:

$$s_{re} = M_0 \frac{\gamma B_1 T_2^2 \Delta\omega}{1 + (\Delta\omega)^2 T_2^2 + (\gamma B_1)^2 T_1 T_2} \tag{22}$$

$$s_{im} = M_0 \frac{\gamma B_1 T_2}{1 + (\Delta\omega)^2 T_2^2 + (\gamma B_1)^2 T_1 T_2}. \tag{23}$$

Eqs. (22) and (23) are the measured signal from a single spin system at steady state in a continuous wave NMR experiment. This solution can also be directly computed using the Bloch equations [5].

Replacing Eq. (13) with the matrices in Eqs. (17), (18), and (20) for a single spin system, and applying the detection method from Eq. (3), we get the measured signal s at the time point b in the x-y plane. Note that, in this case, B_1 is along the y-axis rather than the x-axis and the absorption mode spectra will be the real part of the complex signal.

$$s_{re} = M_0 \frac{e^{-\frac{T_R}{T_2}} \left(1 - e^{-\frac{T_R}{T_1}}\right) \sin(\alpha) \left(\cos(T_R\, \Delta\omega) - e^{-\frac{T_R}{T_2}}\right)}{Q_1} \tag{24}$$

$$s_{im} = -M_0 \frac{e^{-\frac{T_R}{T_2}} \left(1 - e^{-\frac{T_R}{T_1}}\right) \sin(\alpha) \sin(T_R\, \Delta\omega)}{Q_1} \tag{25}$$

where,

$$\begin{aligned} Q_1 = {} & 1 - e^{-\frac{T_R}{T_1}} \cos(\alpha) - e^{-\frac{2T_R}{T_2}} \left(e^{-\frac{T_R}{T_1}} - \cos(\alpha)\right) \\ & - e^{-\frac{T_R}{T_2}} \left(1 - e^{-\frac{T_R}{T_1}}\right) (1 + \cos(\alpha)) \cos(T_R\, \Delta\omega) \end{aligned}$$

Using Eq. (12), we obtain the same magnetization at time point a given by Gyngell [18]. These equations are the full solution for the steady state of pulsed NMR experiments. Note that for each repeat time, the signal is periodic in $\Delta\omega$ with period $1/T_{\mathrm{R}}$.

Substituting the matrices from Eqs. (17), (18), and (20) for a single spin system into Eq. (16), and applying the detection method from Eq. (3), we get the approximate measured signal at the time point b in the x-y plane:

$$s_{re} = M_0 \times \frac{\sin(\alpha) T_{\mathrm{R}} T_2}{T_{\mathrm{R}}^2 + T_{\mathrm{R}}^2 (\Delta\omega)^2 T_2^2 + Q_2} \tag{26}$$

$$s_{im} = -M_0 \times \frac{\sin(\alpha) T_{\mathrm{R}} \Delta\omega T_2^2}{T_{\mathrm{R}}^2 + T_{\mathrm{R}}^2 (\Delta\omega)^2 T_2^2 + Q_2,} \tag{27}$$

where

$$Q_2 = \left(4T_1T_2 + 2T_{\mathrm{R}}(T_1 + T_2) + 2T_1T_2^2T_{\mathrm{R}}(\Delta\omega)^2\right) (\sin(\alpha/2))^2.$$

Eqs. (24), (25), (26), and (27) apply for all flip angles used in SSFP experiments. Carr [9] plots some approximate diagrams when flip angles are over

$\pi/12$ radians.

In order to observe the relation between CW and SSFP solutions, we explore the situation in which the flip angle is very small. In this case, $\sin(\alpha) \approx \alpha$ and $\sin(\alpha/2) \approx \alpha/2$. Considering the relationship, Eq. (8), between the flip angle α and the radio-frequency B_1 field, we get the approximate equations for the signal.

$$s_{re} \approx M_0 \times \frac{\gamma B_1 T_2}{1 + (\Delta\omega)^2 T_2^2 + (\gamma B_1)^2 T_1 T_2 + Q_3} \tag{28}$$

$$s_{im} \approx -M_0 \times \frac{\gamma B_1 \Delta\omega T_2^2}{1 + (\Delta\omega)^2 T_2^2 + (\gamma B_1)^2 T_1 T_2 + Q_3} \tag{29}$$

where,

$$Q_3 = \frac{1}{2}(\gamma B_1)^2 T_{\mathrm{R}}(T_1 + T_2 + T_1 T_2^2 (\Delta\omega)^2)$$

Comparing Eqs. (22) and (29), and Eqs. (23) and (28), if

$$T_{\mathrm{R}} \ll \min\left(\frac{2}{T_1(\gamma B_1)^2}, \frac{2T_1T_2}{T_1 + T_2}\right) \tag{30}$$

the factor Q_3 which broadens the signal can be ignored, Eqs. (28) and (29) will become the same as Eqs. (23) and (22). The real and imaginary parts are swaped because, in this case, the rotation matrix rotates around the y-axis, while the $\mathcal{B}$ matrix acts on the spin system along the x-axis. From the condition on T_{R}, we derive the condition,

$$\alpha \ll \frac{2}{T_1 \gamma B_1}, \tag{31}$$

on the flip angle.

Thus far, solutions for the steady state magnetization in continuous wave and pulsed experiments have been given. The possibility of approximating CW NMR experiments with pulsed steady state experiments for single spin-$\frac{1}{2}$ systems has been explored. Under some conditions, the simulation is very close to the CW NMR experiments. In the next section, we analyze multiple-spin systems.

4 Double-Quantum Transitions of a 2-spin system

In this section, double quantum transitions for coupled spin systems in steady state are discussed. In the Liouville formalism, double-quantum coherence of a 2-spin system is detectable. The double quantum transitions can be obtained by observing the signal of the single quantum transitions at the frequency of $(\omega_{\mathrm{A}} + \omega_{\mathrm{B}})/2$. In this section, we compare different methods of calculating double quantum transitions.

In the previous section, the matrices and vectors for a 1-spin system are listed. Matrices for a 2-spin system can be constructed based on the single spin system. A software package in Maple has been developed to build matrices and vectors for arbitrary spin systems. In this paper, we do not write out the matrices.

4.1 Symbolic Solution of Continuous Wave Experiments

The size of a full basis for a 2-spin system is 16. We do not consider the total magnetization, $|0)|0)$, component, reducing the dimensions of the corresponding matrices $\mathcal{L}, \mathcal{B}, \mathcal{R}$ to 15×15.

Eq. (6) is used to calculate the steady state of CW experiments, but it is difficult to directly compute symbolic ρ_{ss} for a 2-spin system. Maple library functions could not compute a simplified expression, because it was too large. However, forcing simplification at each step of (hand-coded) Gaussian elimination used to solve the system does produce a useful answer.

The following method is used to get the strength of the double quantum transitions of a 2-spin system. The signal ρ_{ss} can be separated into real (ρ_{r}) and imaginary (ρ_{i}) parts. After which the evolution equation

$$(\mathcal{R} + i(\mathcal{L} + \mathcal{B}))(\rho_{\mathrm{r}} + i\rho_{\mathrm{i}}) = \mathcal{R}\rho_{\mathrm{eq}} \tag{32}$$

similarly separates:

$$\mathcal{R}\rho_{\mathrm{r}} - (\mathcal{L} + \mathcal{B})\rho_{\mathrm{i}} = \mathcal{R}\rho_{\mathrm{eq}} \tag{33}$$
$$(\mathcal{L} + \mathcal{B})\rho_{\mathrm{r}} + \mathcal{R}\rho_{\mathrm{i}} = 0 \tag{34}$$

All of the entries of ρ_{eq} are real numbers, so ρ_{eq} represents a real vector. And all of components of the matrices and vectors of the above equations are real. Solving the two equations, we get the following two linear systems:

$$(\mathbf{1} + \mathcal{R}^{-1}(\mathcal{L} + \mathcal{B})\mathcal{R}^{-1}(\mathcal{L} + \mathcal{B}))\rho_{\mathrm{r}} = \rho_{\mathrm{eq}} \tag{35}$$

$$(\mathbf{1} + \mathcal{R}^{-1}(\mathcal{L} + \mathcal{B})\mathcal{R}^{-1}(\mathcal{L} + \mathcal{B}))\rho_{\mathrm{i}} = -\mathcal{R}^{-1}(\mathcal{L} + \mathcal{B})\rho_{\mathrm{eq}} \tag{36}$$

On the other hand, considering the detection of a 2-spin system, we only need the first and fourth components of ρ_{ss} to get the signal of double quantum transitions, so we do not need to get the whole solution of ρ_{ss}. At the same time, the signal of double quantum transitions of a 2-spin system will be at the frequency $(\omega_{\mathrm{A}} + \omega_{\mathrm{B}})/2$ which means that the value of $\Delta\omega$ is 0 in the Liouville matrix $\mathcal{L}$.

A Maple procedure was developed to implement manual Gaussian elimination to solve the new linear systems. Due to the fact that we need only the first and fourth elements, it makes sense to start the Gaussian elimination at the end of the matrix, the fifteenth element. For each step, the pivot was chosen by inspection of the matrix elements, and the Gaussian elimination proceeded. Using this procedure, the signals of double quantum transitions of a 2-spin system in CW experiments (B_1 is along the x-axis.) are:

$$s_{re} = 0 \tag{37}$$

$$s_{im} = M_0 \frac{8T_2\gamma B_1(E_1(\gamma B_1)^2 + T_1^2T_2^2\delta^2 + E_5)}{T_1^2T_2^4\delta^4 + E_2\delta^2 + E_3(\gamma B_1)^4 + E_4(\gamma B_1)^2 + 4E_5} \tag{38}$$

where,

$$\begin{aligned}
E_1 &= 2T_1T_2^2E_6 \\
E_2 &= 8T_1T_2^3 + 8T_1^2T_2^2 + 2T_1T_2^3(2T_1^2 + T_1T_2 + T_2^2)(\gamma B_1)^2 + 4T_2^4 \\
E_3 &= 4T_1T_2E_1 \\
E_4 &= 8T_1T_2(2T_1^2 + 3T_2^2 + 5T_1T_2 + T_1T_2^2(2T_1 + 3T_2)J^2) \\
E_5 &= 4(T_1 + T_2)E_6 \\
E_6 &= T_1T_2^2J^2 + T_1 + T_2
\end{aligned}$$

where J is the coupling constant of spin A and spin B; δ is the difference of Larmor frequencies of spin A and spin B; spin A and spin B have same relaxation times T_1 and T_2. Yatsiv [11] gives the approximate expression, but Eq. (38) is a full solution. Based on this equation, it is easily to observe the relationship of the double quantum transitions with these factors such as the coupling constant, the strength of the rf field, the relax times.

When the coupling constant J is 0, according to Eq. (38), the signal of the

double quantum transition is:

$$s_{imag,J=0} = M_0 \frac{2\gamma B_1 T_2}{1 + T_1 T_2 (\gamma B_1)^2 + (\delta T_2/2)^2} \tag{39}$$

which is the sum of signal of two independent spin systems at the frequency $\frac{\omega_A - \omega_B}{2}$.

When the coupling constant J is going to the infinity, the signal will be:

$$s_{imag,J=\infty} = M_0 \frac{2\gamma B_1 T_2}{1 + T_1 T_2 (\gamma B_1)^2} \tag{40}$$

which is the same as the signal when $\delta = 0$. Please see Fig. (2).

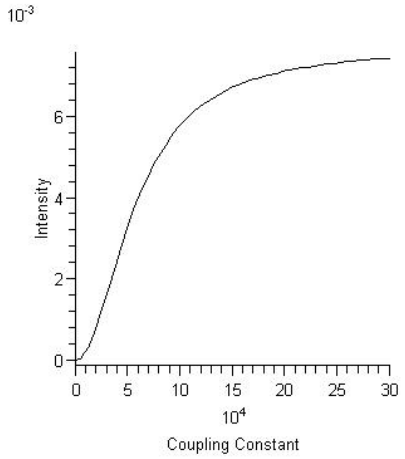

Figure 2. The intensity of the Double Quantum transition at the frequency $\frac{\omega_A + \omega_B}{2}$ is a function of the coupling constant J. Parameters: $\delta_{AB} = 1500$Hz, $T_1 = 0.04$s, $T_2 = 0.02$s, $\gamma B_1 = 0.043478$Hz

Fig. 2 shows that the intensity of the double quantum transitions is going to a constant if the coupling constant is big enough. When the coupling constant is close to 0, the intensity of the double quantum transitions changes very acutely.

When B_1 is zero, the signal will be 0. When B_1 is going to infinity, saturation will appear and the signal will also be 0. Fig. 3 shows the trend.

When substituting J, T_1, T_2 and δ with the parameters of Fig. 3 to Eq. (38), the intensity of the double quantum transition is a function of the variable B_1 as the following:

$$SignalDQ = \frac{7.680101 \times 10^{-5}\, {B_1}^3 + 7.007729\, B_1}{2020634.314 + 0.269143\, {B_1}^2 + 2.172261 \times 10^{-6}\, {B_1}^4} \tag{41}$$

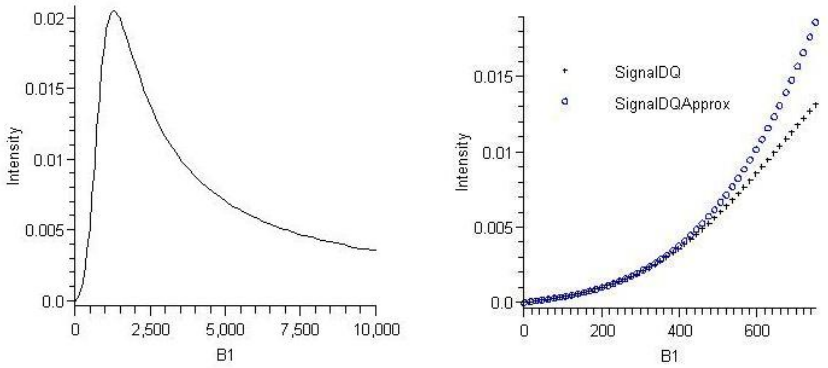

Figure 3. The intensity of the Double Quantum transition at the frequency $\frac{\omega_A+\omega_B}{2}$ is a function of B_1. Parameters: $\delta_{AB} = 1500$Hz, $T_1 = 0.04$s, $T_2 = 0.02$s, $J = 183$Hz

When B_1 is small, the intensity could be approximate by a cubic function:

$$SignalDQApprox = 3.800837 \times 10^{-11}\, {B_1}^3 + 3.468084 \times 10^{-6}\, B_1 \tag{42}$$

When δ is zero, the intensity will be:

$$s_{imag,\delta=0} = M_0 \frac{2\gamma B_1 T_2}{1 + T_1 T_2 (\gamma B_1)^2} \tag{43}$$

When δ is going to infinity, the intensity also will be going to zero. Fig. 4 shows the trend.

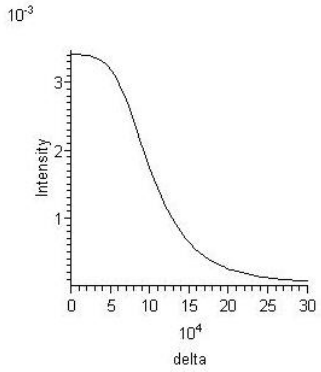

Figure 4. The intensity of the Double Quantum transition is a function of δ. Parameters: $\gamma B_1 = 1650$Hz,$T_1 = 0.04$s,$T_2 = 0.02$s,$J = 183$Hz

Using numerical computation, spectrum can be plotted out by functions Eq. (6) and Eq. (3). The spectra of CW experiments (Fig. 5 and Fig. 6) are plotted out with different parameters so as to show the broadening phenomena.

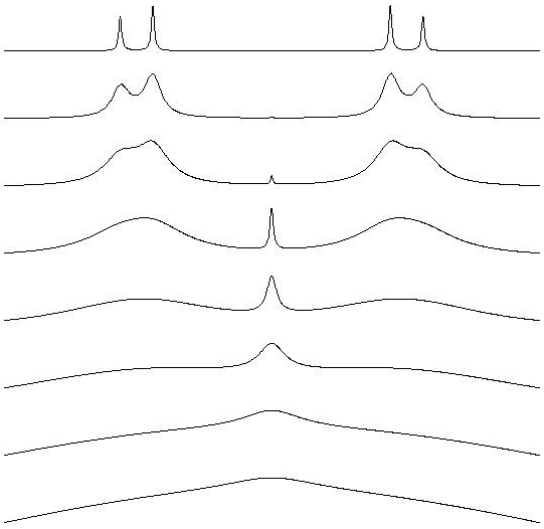

Figure 5. The spectra of a coupled spin system with different $B1$. Parameters: $\delta_{\mathrm{AB}} = 1500\mathrm{Hz}$, $T_1 = 0.04\mathrm{s}$, $T_2 = 0.02\mathrm{s}$, $J = 183\mathrm{Hz}$, $\gamma B_1 = 0.043, 43, 86, 172, 344, 688, 1376, 2173\mathrm{Hz}$

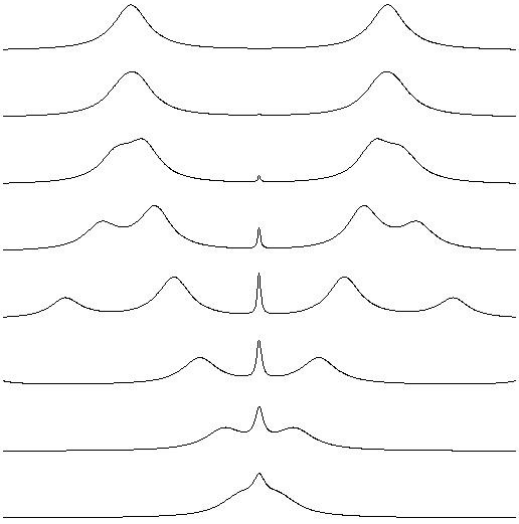

Figure 6. The spectra of a coupled spin system with different coupling constant. Parameters: $\delta_{\mathrm{AB}} = 1500\mathrm{Hz}$, $T_1 = 0.04\mathrm{s}$, $T_2 = 0.02\mathrm{s}$, $\gamma B_1 = 86\mathrm{Hz}$, $J = 0, 80, 160, 320, 640, 1280, 2560, 5120\mathrm{Hz}$

4.2 Numerical Results of Pulsed NMR Experiments

In this subsection, pulsed NMR experiments are used to observe the signal at the frequency $\frac{\omega_{\mathrm{A}}+\omega_{\mathrm{B}}}{2}$ by computing Eq. (13) and Eq. (16). The figures shows that the results of SSFP are very close to CW experiments under small flip angle conditions.

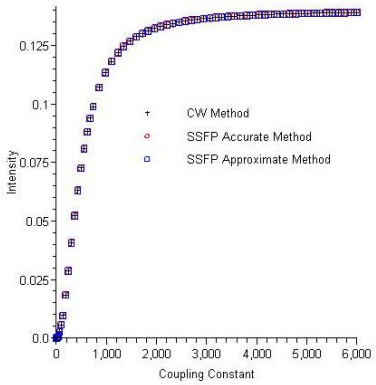

Figure 7. The intensity of the Double Quantum transition is a function of the coupling constant. Parameters: $\delta_{\mathrm{AB}} = 20.69\mathrm{Hz}$, $T_1 = 1\mathrm{s}$, $T_2 = 1\mathrm{s}$, $\alpha = 0.00002\mathrm{rad}$, $T_{\mathrm{R}} = 0.0002\mathrm{s}$, $\gamma B_1 = 0.1\mathrm{Hz}$

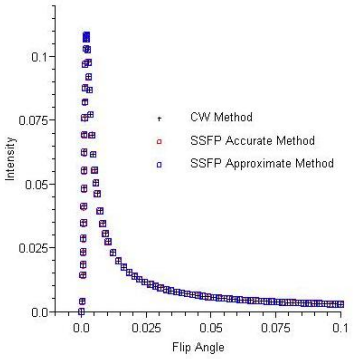

Figure 8. The intensity of the Double Quantum transition is a function of the flip angle. Parameters: $\delta_{\mathrm{AB}} = 20.69\mathrm{Hz}$, $T_1 = 1\mathrm{s}$, $T_2 = 1\mathrm{s}$, $J = 17.38\mathrm{Hz}$, $T_{\mathrm{R}} = 0.0002\mathrm{s}$, $\gamma B_1 = \alpha / T_{\mathrm{R}}$

Fig. 9 shows that error of the accurate and approximation methods will increase along with increase of the repeat time and the flip angle to approximate CW experiments although γB_1 (the rate of the flip angle and the repeat time) is a constant.

5 Extension to multiple spin-$\frac{1}{2}$ systems

Eq. (6), Eq. (13) and Eq. (16) give the general solutions of multiple spin-$\frac{1}{2}$ systems. These equations can be applied to explore the spectrum, multiple quantum transitions, design of pulse sequences, optimization problems. This section shows the feasibility and cost to handle multiple spin systems by the Maple package.

Worvill's figures (Fig. 1-8) [14] have been reproduced by these three methods,

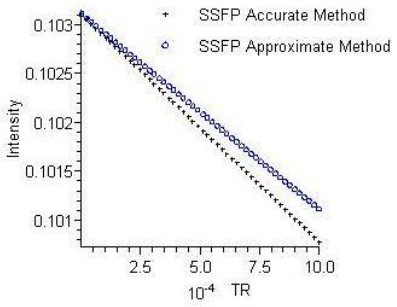

Figure 9. The intensity of the Double Quantum transition is a function of the repeat time and the flip angle of pulses. Parameters: $\delta_{\mathrm{AB}} = 20.69\mathrm{Hz}$, $T_1 = 1\mathrm{s}$, $T_2 = 1\mathrm{s}$, $J = 17.38\mathrm{Hz}$, $\gamma B_1 = \alpha/T_{\mathrm{R}} = 1.30\mathrm{Hz}$

Fig. 10 shows the spectrum by CW method.

Fig. 11 and Fig. 12 display the spectrum of a 4-spin system and a 5-spin system.

When calculating one point of the steady state, Eq. (6) needs to compute a complex matrix inverse one time and the multiplication of a complex matrix and a vector two times; Eq. (13) needs to compute an exponential of a complex matrix one time, the multiplication of a complex matrix and a vector two times, and the addition of matrices two times; Eq. (16) has the same cost as Eq. (6) plus two times' addition of matrices. The computational complexity grows quickly in the Liouville space , since the dimension of the matrices or the eigenvalues for a system of size is 4^n. Table 2 shows the cost for 3-, 4-, 5-spin systems.

System	CW Method	SSFP Accurate Method	SSFP Approximate method
3-spin	56	190	160
4-spin	575	3841	2897
5-spin	10031	102586	52483

Table 2: CPU time (second) of calculating $1k$ points for 3-, 4-, 5-spin systems. The experiments are done on a Power MAC G5 computer, CPU: 2.5GHz, Number of CPUs: 2, Cache: 512Kb×2, RAM: 4G, OS: Mac OS X 10.4.9, Maple: 10.04 (Standard Worksheet Interface)

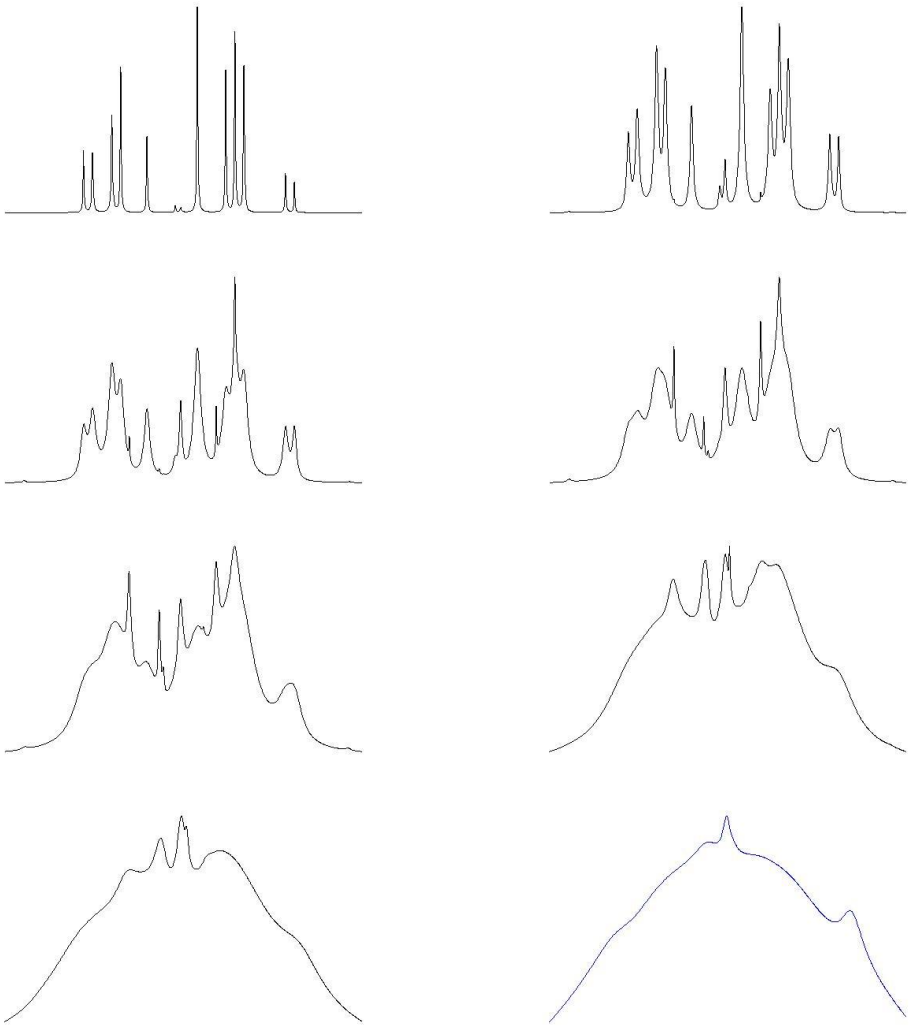

Figure 10. Reproduce Worvill's figures (Fig. 1-8) which are spectrum of a 3-spin system [14] with different B_1. Parameters: $\omega_{\mathrm{A}} = 634.05\mathrm{Hz}$, $\omega_{\mathrm{B}} = 613.36\mathrm{Hz}$, $\omega_{\mathrm{C}} = 583.82\mathrm{Hz}$, $J_{\mathrm{AB}} = 17.38\mathrm{Hz}$, $J_{\mathrm{AC}} = 1.57\mathrm{Hz}$, $J_{\mathrm{BC}} = 10.50\mathrm{Hz}$, $T_1 = 1\mathrm{s}$, $T_2 = 1\mathrm{s}$, $B_1 = 0.1, 10, 20, 4070, 150, 250, 500nT$

6 Conclusion

In this paper, the symbolic solutions of steady state for the single spin system are given. The double quantum transitions of continuous wave experiments is also calculated out by the algebraic computation. A series of spectrum for multiple spin systems are plotted out by different ways. All of these things show that steady state pulsed NMR approximates CW experiments well. The flexibility of our Maple tools allow us to explore more complicated spin systems by CW NMR and pulsed NMR. Along with the increase of number of spins,

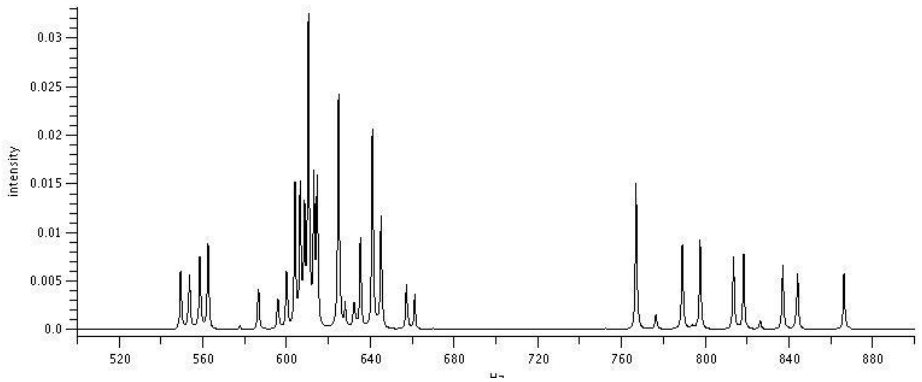

Figure 11. The spectra of a 4-spin system by CW simulation. Parameters: $\omega_{\mathrm{A}} = 634.05$Hz, $\omega_{\mathrm{B}} = 613.36$Hz, $\omega_{\mathrm{C}} = 583.82$Hz, $\omega_{\mathrm{D}} = 812.06$Hz, $J_{\mathrm{AB}} = 17.38$Hz, $J_{\mathrm{AC}} = 1.57$Hz, $J_{\mathrm{AD}} = 30.50$Hz, $J_{\mathrm{BC}} = 10.50$Hz, $J_{\mathrm{BD}} = 20.0$Hz, $J_{\mathrm{CD}} = 50$Hz, $T_1 = 1$s, $T_2 = 1$s, $\gamma B_1 = 0.1$Hz

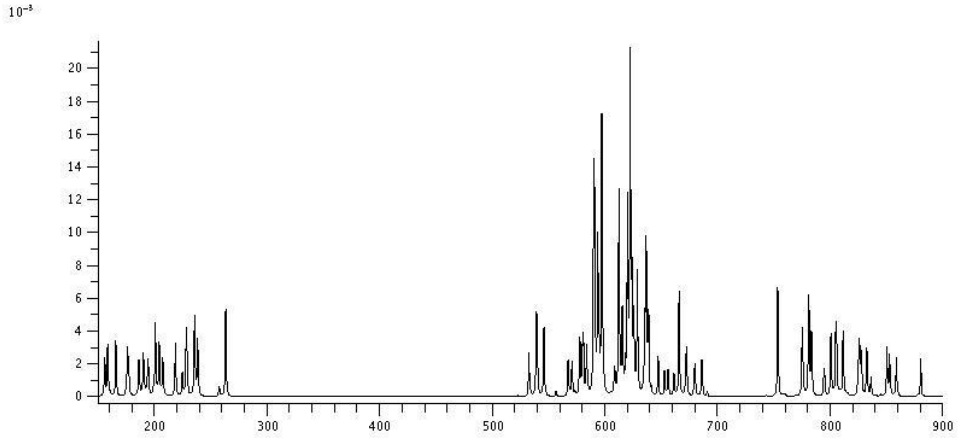

Figure 12. The spectra of a 5-spin system by CW simulation. Parameters: $\omega_{\mathrm{A}} = 634.05$Hz, $\omega_{\mathrm{B}} = 613.36$Hz, $\omega_{\mathrm{C}} = 583.82$Hz, $\omega_{\mathrm{D}} = 812.06$Hz, $\omega_{\mathrm{E}} = 200$Hz, $J_{\mathrm{AB}} = 17.38$Hz, $J_{\mathrm{AC}} = 1.57$Hz, $J_{\mathrm{AD}} = 30.50$Hz, $J_{\mathrm{AE}} = 50$Hz, $J_{\mathrm{BC}} = 10.50$Hz, $J_{\mathrm{BD}} = 20.0$Hz, $J_{\mathrm{BE}} = 20$Hz, $J_{\mathrm{CD}} = 50$Hz, $J_{\mathrm{CE}} = 35$Hz, $J_{\mathrm{DE}} = 28$Hz, $T_1 = 1$s, $T_2 = 1$s, $\gamma B_1 = 0.1$Hz

the computational complexity grows quickly, so some numerical methods such as BLAS, sparse matrix technique should be applied to improve the efficiency.

Acknowledgment: Alex D. Bain would like to thank the Natural Science and Engineering Research Council of Canada (NSERC) for financial support.

References

[1] C. Ganter, Steady state of gradient echo sequences with radiofrequency phase cycling: Analytical solution, contrast enhancement with partial spoiling, Magnetic Resonance in Medicine 55 (1) (2006) 98–107.

[2] E. M. Haacke, R.W. Brown, M.R. Thompson, R. Venkatesan, Magnetic resonance imaging : physical principles and sequence design, Wiley-Liss, New York, 1999.

[3] W. Hanicke, H. U. Vogel, An analytical solution for the ssfp signal in MRI, Magnetic Resonance in Medicine 49 (4) (2003) 771–775.

[4] F. Bloch, Nuclear induction, Phys.Rev. 70 (7–8) (1946) 460–474.

[5] A. Carrington, A. D. McLachlan, Introduction to magnetic resonance with applications to chemistry and chemical physics, Harper's chemistry series, Harper & Row, New York, 1967.

[6] R. Freeman, H. D. W. Hill, Phase and intensity anomalies in Fourier transform NMR, Journal of Magnetic Resonance (1969) 4 (3) (1971) 366–383.

[7] J. A. Pople, W.G. Schneider, H.J. Bernstein, High-resolution nuclear magnetic resonance, McGraw-Hill series in advanced chemistry, McGraw–Hill, New York, 1959.

[8] P. Waldstein, W. E. Wallace, Jr, Driven equilibrium methods for enhancement of nuclear transients, Review of Scientific Instruments 42 (4) (1971) 437–440.

[9] H. Y. Carr, Steady-state free precession in nuclear magnetic resonance, Phys. Rev. 112 (5) (1958) 1693–1701.

[10] W. A. Anderson, R. Freeman, C. A. Reilly, Assignment of NMR spectra with the aid of double-quantum transitions, The Journal of Chemical Physics 39 (6) (1963) 1518–1531.

[11] S. Yatsiv, Multiple-quantum transitions in nuclear magnetic resonance, Phys.Rev. 113 (6) (1959) 1522–1537.

[12] J. I. Kaplan, S. Meiboom, Double-quantum transitions in nuclear magnetic resonance spectra of liquids, Phys. Rev. 106 (3) (1957) 499–501.

[13] J. I. Musher, Role of multiple quantum transitions in NMR: A three-spin system, The Journal of Chemical Physics 40 (4) (1964) 983–990.

[14] K. M. Worvill, The NMR multiple quantum spectrum of a three-spin system, Journal of Magnetic Resonance (1969) 18 (2) (1975) 217–229.

[15] A. D. Bain, J. S. Martin, FT NMR of nonequilibrium states of complex spin systems. I. a Liouville space description, Journal of Magnetic Resonance (1969) 29 (1) (1978) 125–135.

[16] U. Fano, Lectures on the many-body problem, volume 2, Edited by E. R. Caianiello. Published by Academic Press, New York, 1964.

[17] R. N. Zare, Angular momentum : understanding spatial aspects in chemistry and physics, George Fisher Baker non-resident lectureship in chemistry at Cornell University., Wiley, New York, 1988.

[18] M. L. Gyngell, The steady-state signals in short-repetition-time sequences, Journal of Magnetic Resonance (1969) 81 (3) (1989) 474–483.

[19] C. K. Anand, A. D. Bain, Z. Nie, The simulation and optimization of pulsed NMR experiments using a liouville space method, in: The Maple Conference, Waterloo,Canada, 2006, pp. 123–135,.

[20] G. Bodenhausen, Multiple-quantum NMR, Progress in Nuclear Magnetic Resonance Spectroscopy 14 (3) (1980) 137–173.

[21] B. A. Hargreaves, S. S. Vasanawala, J. M. Pauly, D. G. Nishimura, Characterization and reduction of the transient response in steady−state MR imaging, Magnetic Resonance in Medicine 46 (1) (2001) 149–158.

[22] W. S. Hinshaw, Image formation by nuclear magnetic resonance: The sensitive-point method, Journal of Applied Physics 47 (8) (1976) 3709–3721.

[23] K. Scheffler, On the transient phase of balanced ssfp sequences, Magnetic Resonance in Medicine 49 (4) (2003) 781–783.

[24] K. Scheffler, A pictorial description of steady–states in rapid magnetic resonance imaging, Concepts in Magnetic Resonance 11 (5) (1999) 291–304.